



ARTICLE

Conductive Polymer Composites Fabricated by Disposable Face Masks and Multi-Walled Carbon Nanotubes: Crystalline Structure and Enhancement Effect

Meng Xiang¹, Zhou Yang¹, Jingjing Yang¹, Tong Lu¹, Danqi Wu¹, Zhijun Liu¹, Rongjie Xue¹ and Shuang Dong^{2,*}

¹Department of Materials Engineering, Jiangsu University of Technology, Changzhou, 213001, China

²Department of Mathematics Science and Chemical Engineering, Changzhou Institute of Technology, Changzhou, 213032, China

*Corresponding Author: Shuang Dong. Email: dongs@czu.cn

Received: 03 May 2021 Accepted: 15 June 2021

ABSTRACT

Influenced by recent COVID-19, wearing face masks to block the spread of the epidemic has become the simplest and most effective way. However, after the people wear masks, thousands of tons of medical waste by used disposable masks will be generated every day in the world, causing great pressure on the environment. Herein, conductive polymer composites are fabricated by simple melt blending of mask fragments (mask polypropylene, short for mPP) and multi-walled carbon nanotubes (MWNTs). MWNTs were used as modifiers for composites because of their high strength and high conductivity. The crystalline structure, mechanical, electrical and thermal enhancement effect of the composites were investigated. MWNTs with high thermal stability acted the role of promoting the crystallisation of mPP by expediting the crystalline nucleation, leading to the improvement of amount for crystalline nucleus. MWNTs fibers interpenetrate with each other in mPP matrix to form conducting network. With 2.0 wt% MWNTs loading, the tensile strength and electrical conductivity of the composites were increased by 809% and 7 orders of magnitude. MWNTs fibers interpenetrate with each other in mPP matrix to form conducting network. Thus, more conducting paths were constructed to transport carriers. The findings may open a way for high value utilization of the disposable masks.

KEYWORDS

Disposable face masks; multi-walled carbon nanotubes; crystalline structure; mechanical enhancement effect; conducting network

1 Introduction

Influenced by recent COVID-19, wearing face masks to block the spread of the epidemic has become the simplest and most effective way [1]. However, after the people wear masks, there are also some inevitable but not enough attention to follow-up problems, among which the most important is how to deal with the used disposable masks. If the average weight of a common three-layer disposable mask is 5 g, thousands of tons of medical waste will be generated every day in the world, causing great pressure on the environment [2]. The structure of the common disposable mask is divided into three parts: the mask body, the ear straps and nose seals. The mask body is a non-woven fabric composed of high fluidity polypropylene (PP) resin, the ear straps were elastomer composed of polyurethane, and the nose seals were composed of iron wire and



polypropylene resin. In addition to the fact that the nose seals are difficult to be reused because of the iron wire, polymer composites with high performance and high added value could be easily prepared by using the structural characteristics of the rest parts of the disposable mask, which has good ecological and economic benefits, and is helpful to solve the problems of environmental pollution and resource shortage in our society.

For the primitive polymer materials, the surface resistivity range is within 10^{12} – 10^{14} Ω , which easily leads to the build-up of static charge on the surface of polymer materials, as well as the dust contamination, short circuit and even cause a fire or an explosion in explosive, mining equipment, packaging of electrical devices and so on [3]. Therefore, conductive composites with improved antistatic property were required in those areas [4]. Compared with conductive metal composites, conductive polymer composites have lower density, better flexibility, simpler preparation and lower cost [5]. However, traditional conductive polymer composites are usually made of raw materials from petrochemical resources, which consume a lot of non-renewable petrochemical resources. If the raw material used in the study was neat PP, the increase of tensile strength of the composites was limited [6]. High molecular weight of neat PP leads to high melt viscosity in the preparation of the composites, in which the MWNTs would be more difficult to uniformly dispersed in neat PP matrix, leading to a poor increase of mechanical property of the composites. On the other hand, compared with neat PP, the molecular weight of the recycled PP decreases due to thermal oxidative degradation, leading to the lower melt viscosity in the preparation of the composites, in which the MWNTs would be easier to uniformly dispersed in recycled PP matrix, leading to a higher increase of mechanical property of the composites. At present, researchers have made some progress in this field of high value utilization of recycled PP and recycled fillers: Belviso et al. [7] investigated a rapid recycling method of waste polypropylene (WPP) from automotive industry with the addition of recycled inorganic fillers. The results indicate that the addition of low percentage (5.0 wt%) of sepiolite or zeolite improves tensile modulus of WPP-recycled materials by 5.4%. Ajourloo et al. [8] incorporated of recycled PP and wasted fly ash in PP-based composites for automotive applications. The impact strength of the recycled composites increased by 23.3% under 30.0 wt% fly ash. Bahri et al. [9] fabricated functionally graded natural filler-recycled polypropylene (FGNF-RPP) composite and investigated deflection behaviour under static mechanical loads. The results showed that composite under 40.0 wt% waste wood sawdust produced the least deflection. Barczewski et al. [10] produced polymer composites based on recycled PP incorporating ground sunflower husk. The elasticity modulus of the green composites was increased by 19.4% in the filler amount of 20.0 wt%. Battegazzore et al. [11] proposed a mechanical recycling protocol of disposable masks by directly melt blending the mask body with ear straps. However, The Young's Modulus and maximum stress of the composites were decreased with the ear straps loading compared with only use mask body.

The focus of recent researches has been mostly on the effect of reprocessing on the mechanical properties of recycled commercial PP and different fillers. However, very few publications are available in the literature that discusses the electrically or thermally conductive properties of recycled PP from disposable face masks. In this research, conductive polymer composites are fabricated by simple melt blending of mask fragments (mask polypropylene, short for mPP) and multi-walled carbon nanotubes (MWNTs). At our processing temperature of 180°C, the COVID-19 virus will be quickly inactivated [12]. MWNTs were used as modifiers for composites because of their high strength and high conductivity. The crystalline structure, mechanical, electrical and thermal enhancement effect of the composites were investigated. To the best of the authors' knowledge, this is the first study investigating the electrically and thermally conductive properties of the green composites from disposable mask fragments. The obtained composites could be applied to the fields of sustainable railway sleepers [13], 3D printing feedstock materials [14] and low value building materials [15]. The importance of this research gets highlighted when we consider that the reuse of disposable mask fragments may be an

environmental and economic solution, which could help to the efficient elimination of waste materials from the biosphere to some extent.

2 Experimental

2.1 Materials

The disposable mask (Henan Chaoya) and MWNTs (Huizhou Tannatong) were purchased. After removed nose seals and ear straps, the disposable mask was smashed into mask fragments (mask polypropylene, short for mPP).

2.2 Preparation

Firstly, the polypropylene fabric was directly compressed at 180°C for 5 min after removing nose seals and ear straps, as shown in Fig. 1a. After that, we cut the compressed products into small pieces with scissors, as shown in Fig. 1b. Finally, we added the small pieces of polypropylene fabric (mPP) in to the internal mixer at 180°C for 5 min again for the preparation of the mPP/MWNTs composites (Fig. 1c).



Figure 1: Compressing (a), cutting (b) and feeding (c) of mPP

The mPP were mixed with MWNTs at 180°C for 5 min. After that, the composites were prepared by compressing the mixed products at 180°C for 5 min again (Fig. 2). The samples were named as mPP/Xwt% MWNTs, in which X denotes MWNTs content in the composites.

2.3 Measurements

The Fourier-transform infrared (FT-IR), Non-Isothermal Crystallization DSC Analysis, X-ray diffraction (XRD), Thermal gravimetric analysis (TGA), scanning electron microscope (SEM), mechanical and electrical performance testing of the samples were similar to our preliminary theses [16,17]. Besides, the melt flow index of samples was tested by a SANS ZRZ1452 melt flow indexer (MFI) (China), the testing temperature was 166°C and the loading weight was 2.16 kg. The tensile performance of the samples was measured with a 4302 material testing machine from Instron Co., (USA), according to ISO 527-1993. The tensile test speed was 10 mm/min, and the sample length between bench

marks was 25 ± 0.5 mm. The notched impact strength of the samples was measured with ZBC-4B impact testing machine from Xinsansi Co. (Shenzhen,China) according to ISO 179-1993 standards. The electrical conductivity of the samples was measured with ZC36 high insulation resistance meter spectrometer (China). The thermal conductivity of the samples was calculated from the thermal diffusivity which was measured by using a NETZSCH-LFA 447 instrument.

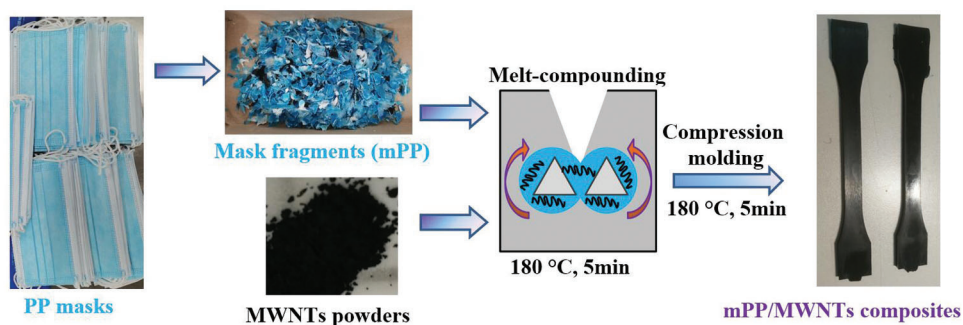


Figure 2: Preparation of mPP/MWNTs composites

3 Results and Discussion

The influence of the recycling of the PP due to chain scission could be deduced from the melt flow index (MFI) of the samples, as shown in Fig. 3. The primitive face mask in this paper denotes the sample of disposable face masks determining MFI after been cut into small pieces with scissors directly, without been compressed at 180°C for 5 min and internal mixed at 180°C for 5 min again. Through the comparison of primitive face mask and mPP in MFI determination, we can see the influence of hot pressing and internal mixing on the fluidity of polymer. When primitive face masks were processed into mPP, the change of MFI was not obvious due to the low speed (50 rpm) of melt processing in the torque rheometer. Therefore, chain scission did not occur in this processing. However, the MFI of the composites rapidly decreased with MWNTs loading, indicating that the MWNTs fillers with large aspect ratio would reduce the melt fluidity of composites.

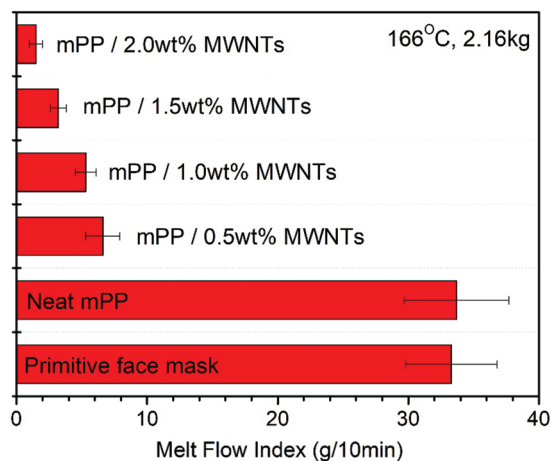


Figure 3: MFI of neat mPP and mPP/MWNTs composites

Fig. 4 displays the FT-IR curves of Neat mPP and mPP/MWNTs composites. Neat mPP exhibits typical peaks at 1458 cm^{-1} ($-\text{CH}_3$ asymmetric deformation vibration), 1374 cm^{-1} ($-\text{CH}_3$ symmetric deformation vibration). And the peaks at 1152 cm^{-1} (C-C stretching vibration in propylene chains), 973 cm^{-1} ($-\text{CH}_3$ symmetric rocking vibration) demonstrate the head to tail structure in mPP chains [18]. For mPP/MWNTs composites, caused by the shielding effect of carbon hexatomic ring of MWNTs in infrared band, the peak intensity ascribed to mPP are weakened as the MWNTs loading [19]. Furthermore, there was no absorption peak of carbonyl group at 1716 cm^{-1} in the infrared spectra of all samples, which indicated that the samples did not undergo thermal oxidative degradation during the processing of this study.

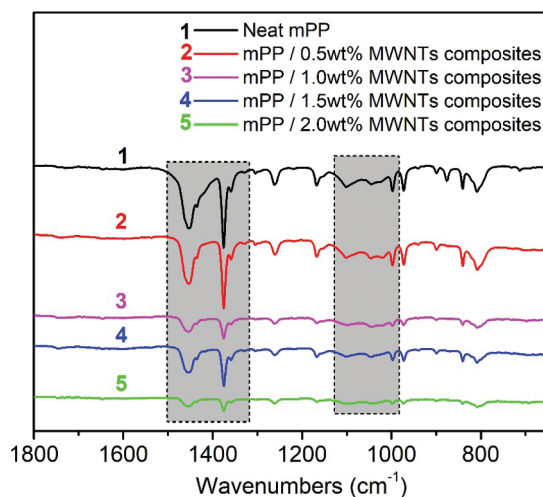


Figure 4: FT-IR curves of neat mPP and mPP/MWNTs composites

The thermal stability of Neat mPP and mPP/MWNTs composites are listed in Fig. 5a. For Neat mPP, the degradation stage during $380\text{--}450^\circ\text{C}$ was due to fracture of C-C bond in mPP chains. The thermal stability of mPP/MWNTs composites are enhanced in the same degradation stage, and the ultimate weight loss of mPP/MWNTs composites was fewer compared with Neat mPP. As shown in Fig. 5b, the corresponding DTG results obtained shown that the initial decomposing temperature and maximum decomposing temperature of mPP are postponed and the exothermic rate is retarded with adding the thermal stabilizer of MWNTs. The enhanced thermal stability of the composites come from the good thermal stability of the MWNTs their selves. Besides, good thermal conductivity of MWNTs can transfer the heat needed by the thermal decomposition of the composite in time.

The non-isothermal DSC results such as crystallization temperature (T_c), the melting temperature (T_m), the half peak width (ΔW), and the crystallinity (X_c , DSC) of Neat mPP and mPP/MWNTs composites could be deduced from Figs. 6a and 6b, and were organized in Tab. 1 [20].

The change of T_m and ΔW of the composites was slight; however, T_c of the composites improves with the MWNTs loading. The super cooling degree ($T_m - T_c$) continues declining. The crystallinity (X_c) of the composites presents the same tendency with T_c , indicating the nucleation effect of MWNTs on mPP as heterogeneous nucleating agents.

XRD results were placed in Fig. 7. Neat mPP indicated summits of crystalline form α at $2\theta = 14.4^\circ$, 17.3° , 19.2° , 22.4° and 30.1° , corresponding to the (110), (040), (130), (131), (041) and (111) planes, respectively. mPP/MWNTs composites shows different diffraction peaks at $2\theta = 26.1^\circ$ corresponding to (002) plane of carbon hexatomic ring, indicating the successful introduction of MWNTs in the matrix.

Besides, the introduction of MWNTs promotes the growth of mPP crystals along (110) and (040) planes, resulting from the heterogeneous nucleation effect of MWNTs from crystal lattice in the composites [21].

The degree of crystallinity (X_c , XRD) and crystallized grain sizes (L_{hkl}) could be obtained via:

$$X_c, XRD = (I_c / (I_c + I_a)) \times 100\% \quad (1)$$

where I_c was the area contained in crystallization lines while I_a was the area contained in amorphous lines.

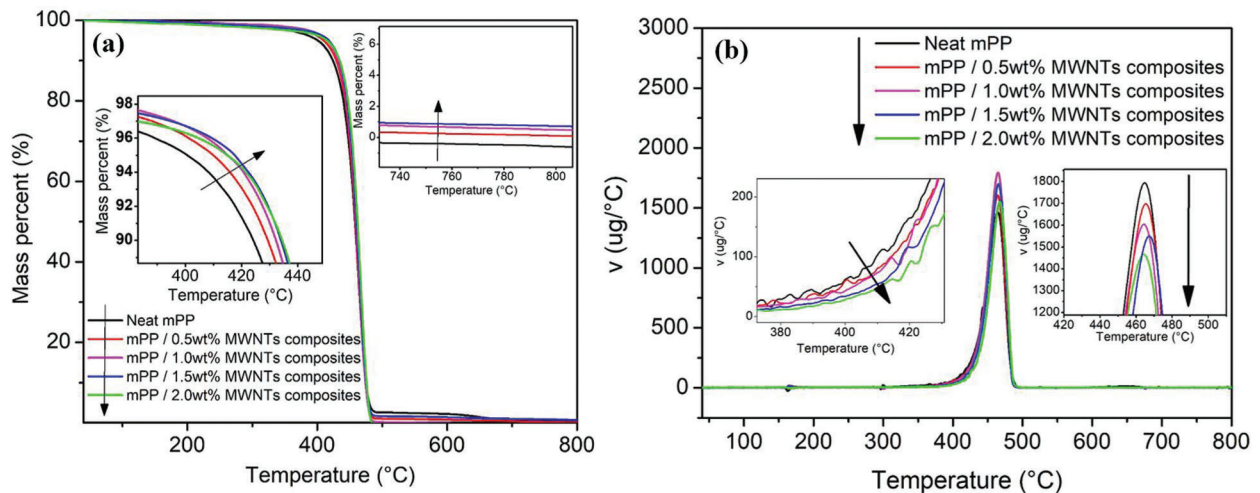


Figure 5: TG (a) and DTG (b) curves of neat mPP and mPP/MWNTs composites

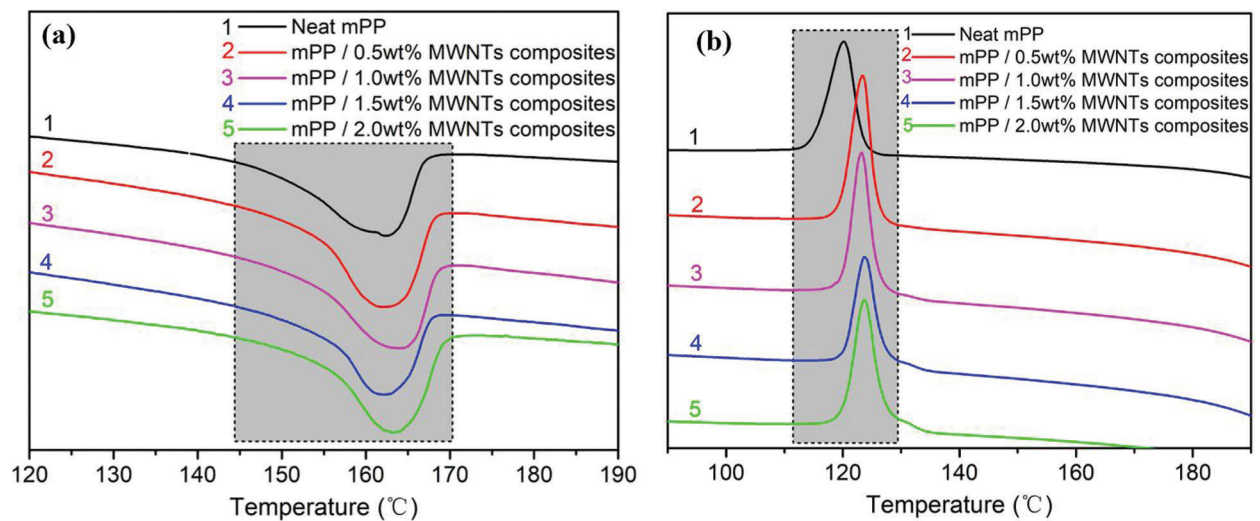


Figure 6: Non-isothermal DSC curves of mPP/MWNTs composites

Formula of Scherrer

$$L_{hkl} = k\lambda/(\beta\cos\theta) \quad (2)$$

where L_{hkl} was the size of crystalline grains in normal direction from hkl planes; k was constant of Scherrer ($k = 0.89$); λ was length of diffraction wave, about 0.154 nm while β was full width of half maximum of the diffraction peak (hkl); θ was angle of Bragg.

For results in [Tab. 1](#), the crystallinity of the composites kept improving with MWNTs loading, being consistent with non-isothermal DSC results, however, the crystalline grains size of the composites shows opposite rule of change. MWNTs acted the role of promoting the crystallisation of mPP by expediting the crystalline nucleation, leading to the improvement of amount for crystalline nucleus. Thus, grain size turns smaller by MWNTs loading.

Table 1: Non-isothermal DSC and XRD parameters of mPP/MWNTs composites with varying MWNTs content

MWNTs content (wt%)	T_m (°C)	$T_m - T_c$ (°C)	T_c (°C)	ΔW (°C)	$X_{c, DSC}$ (%)	$X_{c, XRD}$ (%)	Grain size in (040) plane (nm)
0	161.5	41.4	120.1	8.6	42.6	51.2	14.3
0.5	162.5	38.7	123.8	6.5	47.0	58.3	12.0
1.0	162.9	38.8	124.1	6.7	48.4	66.7	11.3
1.5	164.7	40.0	124.7	6.2	50.1	69.0	10.4
2.0	164.1	39.2	124.9	6.5	51.7	73.2	9.5

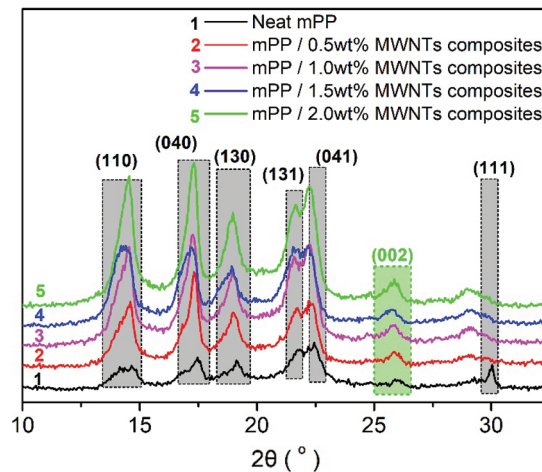


Figure 7: XRD curves of mPP/MWNTs composites

In [Fig. 8a](#), the stress-strain curves of all samples showed a brittle fracture property without any yield points. The strength of mPP/MWNTs composites enhance with increasing of MWNTs contents. The areas contained in stress-strain lines improved drastically compared to neat mPP, denoting the improving toughness of mPP/MWNTs composites. [Figs. 8b–8d](#) tell the mechanical properties of mPP/MWNTs

composites with various MWNTs loading. The tensile strength of the composites increase gradually as MWNTs loading, reaching the maximum of 34.03 MPa (increased by 809%) at 2.0 wt% MWNTs, which was higher than common commercial grade polypropylene (such as 30.5 MPa of T30S). The elongation at break of the composites also presented similar rule with impact strength, also meaning the toughening effects of cellulose skeleton of MWNTs on mPP matrix. The Young's modulus of the composites increased slowly and gradually stabilized with MWNTs loading. Caused by the high aspect ratio and high rigidity of MWNTs themselves, the ability of the composite to resist elastic deformation is enhanced. To sum up, our research shows a certain practical value in terms of mechanical enhancement.

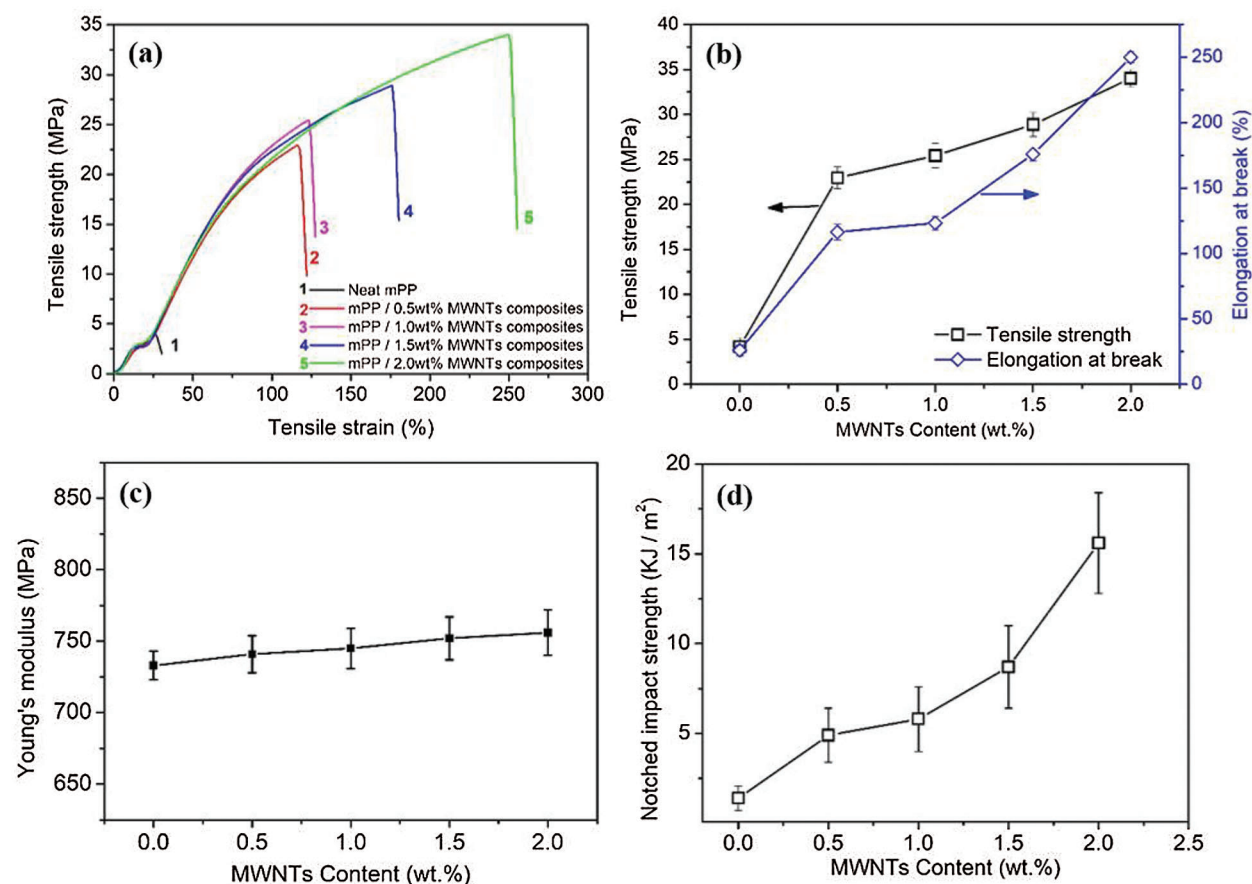


Figure 8: Mechanical properties (a–d) of neat mPP and mPP/MWNTs composites

Fig. 9a shows electrical conductivity of the composites by different MWNTs content. The conductivity of Neat mPP was 1.6×10^{-15} S/m. However, the conductivity in mPP/MWNTs composites improves by MWNTs contents, while the percolation threshold was under 1.0 wt%. By MWNTs contents of 2.0 wt%, composite owns conductivity of 2.7×10^{-8} S/m, suggesting the final formation of the conducting network in mPP matrix. The thermal conductivity of composites improves by MWNTs loading (Fig. 9b). The thermal conductivity of the composites containing 2.0 wt% MWNTs improves by 33%. Herein, MWNTs were dispersed uniformly in highly fluid mPP matrix, leading to the available thermal energy transfer alongside the conducting network.

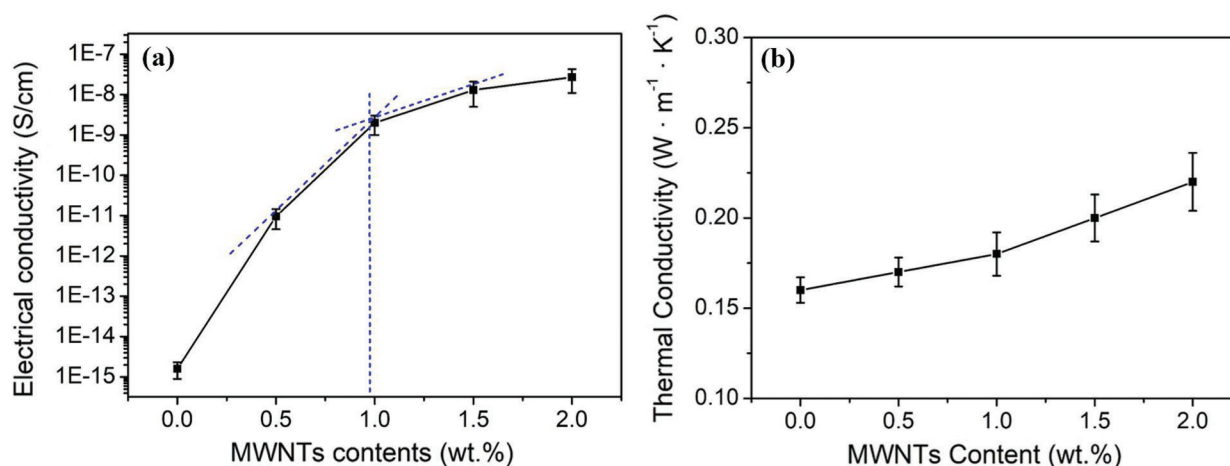


Figure 9: Electrical properties (a) and thermal properties (b) of neat mPP and mPP/MWNTs composites

When observed by the SEM of the fractures of the samples made at low magnification, as shown in Fig. 10a, there is no defect in the Neat mPP, demonstrating the correct preparation of the polymer composition. In Fig. 10b, the tensile fracture surface of mPP/2.0 wt% MWNTs composites was observed with SEM. It could be observed that MWNTs were uniformly dispersed in PP matrix. Firstly, just as the graphene, MWNTs were composed of hexagonal carbon atoms with low polarity, which has good compatibility with PP owning similarly low polarity [22]. Secondly, the recycled mPP from disposable face masks has a relatively small molecular weight, leading to the lower melt viscosity in the preparation of the composites, in which the MWNTs can be easier to uniformly dispersed in recycled PP matrix.

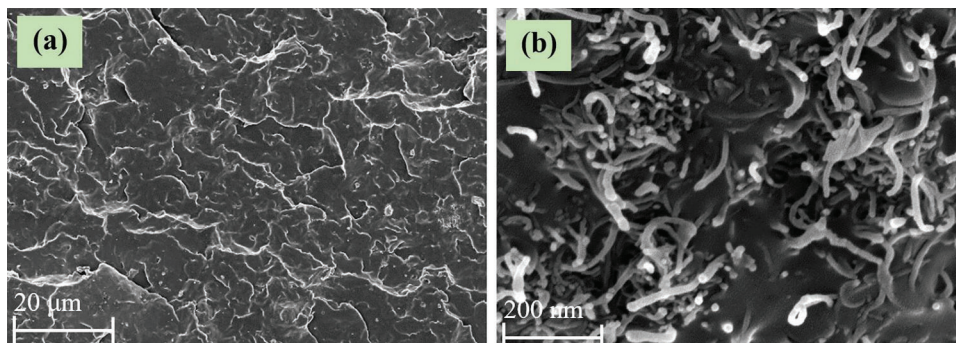


Figure 10: SEM image of tensile fracture surface of neat mPP (a) and mPP/2.0 wt% MWNTs composites (b)

Besides, the outer wall of pulled out MWNTs from mPP matrix is rough, attached with a large amount of mPP fragments, suggesting that there is a strong interfacial interaction between mPP and MWNTs. Moreover, MWNTs fibers interpenetrate with each other in mPP matrix to form conducting network. Thus, more conducting paths were constructed to transport carriers, and mPP matrix is locked in the conducting network to avoid rupture under strong external force, coincide with the mechanical and conducting properties.

4 Conclusions

Conductive polymer composites are fabricated by simple melt blending of mPP and MWNTs. The mechanical and electrical enhancement effect of the composites were investigated. In FT-IR analysis,

caused by the shielding effect of carbon hexatomic ring of MWNTs in infrared band, the peak intensity ascribed to mPP are weakened as the MWNTs loading. TG denotes that the enhanced thermal stability of the composites results from MWNTs themselves. DSC and XRD indicated that MWNTs acted the role of promoting the crystallisation of mPP by expediting the crystalline nucleation, leading to the improvement of amount for crystalline nucleus. The tensile strength of the composites increase gradually as MWNTs loading, reaching the maximum of 34.03 MPa (increased by 809%) at 2.0 wt% MWNTs, which was higher than common commercial grade polypropylene (such as 30.5 MPa of T30S). MWNTs fibers interpenetrate with each other in mPP matrix to form conducting network. Thus, more conducting paths were constructed to transport carriers, and mPP matrix is locked in the conducting network to avoid rupture under strong external force, leading to the improved mechanical, electrical and thermal properties of the composites.

Funding Statement: M. Xiang and S. Dong wishes to thank the National Natural Science Foundation of China (21908086 and 51801083), Changzhou Sci & Tech Program (CJ20190035), Jiangsu Higher Education Institutions in China (19KJB610011) and Natural Science Foundation of Jiangsu Province (BK20181044).

Conflicts of Interest: The authors declare that they have no conflicts of interest to report regarding the present study.

References

1. Abboah-Offei, M., Salifu, Y., Adewale, B., Bayuo, J., Ofosu-Poku, R. et al. (2021). A rapid review of the use of face mask in preventing the spread of COVID-19. *International Journal of Nursing Studies Advances*, 3, 100013. DOI 10.1016/j.ijnsa.2020.100013.
2. Anastopoulos, I., Pashalidis, I. (2021). Single-use surgical face masks, as a potential source of microplastics: Do they act as pollutant carriers? *Journal of Molecular Liquids*, 326(3), 115247. DOI 10.1016/j.molliq.2020.115247.
3. Wang, M., Tang, X. H., Cai, J. H., Wu, H., Shen, J. B. et al. (2021). Fabrication, mechanisms and perspectives of conductive polymer composites with multiple interfaces for electromagnetic interference shielding: A review. *Carbon*, 177, 377–402. DOI 10.1016/j.carbon.2021.02.047.
4. Tang, L. P., Yang, S., Liu, D., Wang, C., Ge, Y. Q. et al. (2020). Two-dimensional porous coordination polymers and nano-composites for electrocatalysis and electrically conductive applications. *Journal of Materials Chemistry A*, 8(29), 14356–14383. DOI 10.1039/D0TA03356A.
5. Gao, J. F., Wang, L., Guo, Z., Li, B., Wang, H. et al. (2020). Flexible, superhydrophobic, and electrically conductive polymer nanofiber composite for multifunctional sensing applications. *Chemical Engineering Journal*, 381, 12. DOI 10.1016/j.cej.2019.122778.
6. Stanciu, N. V., Stan, F., Sandu, I. L., Fetecau, C., Turcanu, A. M. (2021). Thermal, Rheological, mechanical, and electrical properties of polypropylene/multi-walled carbon nanotube nanocomposites. *Polymers*, 13(2), 22. DOI 10.3390/polym13020187.
7. Belviso, C., Montano, P., Lettino, A., Toschi, F., Guarnaccio, A. (2021). Determining the role of the method used to recycle polypropylene waste materials from automotive industry using sepiolite and zeolite fillers. *Journal of Material Cycles and Waste Management*, 23(3), 965–975. DOI 10.1007/s10163-021-01184-w.
8. Ajorloo, M., Ghodrat, M., Kang, W. H. (2021). Incorporation of recycled polypropylene and fly ash in polypropylene-based composites for automotive applications. *Journal of Polymers and the Environment*, 29(4), 1298–1309. DOI 10.1007/s10924-020-01961-y.
9. Bahri, M. A. S., Ratnam, M. M., Khalil, H. (2020). Functionally graded wood filler-recycled polypropylene composite: Effect of mechanical loading on deflection of cantilever beam. *Advanced Composites Letters*, 29(2), 9. DOI 10.1177/2633366X20922856.
10. Barczewski, M., Andrzejewski, J., Majchrowski, R., Dobrzycki, K., Formela, K. (2021). Mechanical properties, microstructure and surface quality of polypropylene green composites as a function of sunflower husk waste filler particle size and content. *Journal of Renewable Materials*, 9(5), 841–853. DOI 10.32604/jrm.2021.014490.

11. Battezzore, D., Cravero, F., Frache, A. (2020). Is it possible to mechanical recycle the materials of the disposable filtering masks? *Polymers*, 12(11), 18. DOI 10.3390/polym12112726.
12. Wu, Z. G., Zheng, H. Y., Gu, J., Li, F., Lv, R. L. et al. (2020). Effects of different temperature and time durations of virus inactivation on results of real-time fluorescence PCR testing of COVID-19 viruses. *Current Medical Science*, 40(4), 614–617. DOI 10.1007/s11596-020-2224-y.
13. Ju, S., Yoon, J., Sung, D., Pyo, S. (2020). Mechanical properties of coal ash particle-reinforced recycled plastic-based composites for sustainable railway sleepers. *Polymers*, 12(10), 15. DOI 10.3390/polym12102287.
14. Carrete, I. A., Quinonez, P. A., Bermudez, D., Roberson, D. A. (2021). Incorporating textile-derived cellulose fibers for the strengthening of recycled polyethylene terephthalate for 3D printing feedstock materials. *Journal of Polymers and the Environment*, 29(2), 662–671. DOI 10.1007/s10924-020-01900-x.
15. Echeverria, C. A., Pahlevani, F., Sahajwalla, V. (2020). Valorisation of discarded nonwoven polypropylene as potential matrix-phase for thermoplastic-lignocellulose hybrid material engineered for building applications. *Journal of Cleaner Production*, 258(54), 11. DOI 10.1016/j.jclepro.2020.120730.
16. Xiang, M., Xu, S., Li, C. J., Ye, L. (2016). Monomer casting nylon-6-b-polyether amine copolymers: Synthesis and antistatic property. *Polymer Engineering and Science*, 56(7), 817–828. DOI 10.1002/pen.24310.
17. Xiang, M., Yang, R., Yang, J., Zhou, S., Zhou, J. et al. (2019). Fabrication of polyamide 6/reduced graphene oxide nano-composites by conductive cellulose skeleton structure and its conductive behavior. *Composites Part B: Engineering*, 167, 533–543. DOI 10.1016/j.compositesb.2019.03.033.
18. Gopanna, A., Mandapati, R. N., Thomas, S. P., Rajan, K., Chavali, M. (2019). Fourier transform infrared spectroscopy (FTIR), Raman spectroscopy and wide-angle X-ray scattering (WAXS) of polypropylene (PP)/cyclic olefin copolymer (COC) blends for qualitative and quantitative analysis. *Polymer Bulletin*, 76(8), 4259–4274. DOI 10.1007/s00289-018-2599-0.
19. Wang, P. H., Ghoshal, S., Gulgunje, P., Verghese, N., Kumar, S. (2016). Polypropylene nanocomposites with polymer coated multiwall carbon nanotubes. *Polymer*, 100(2), 244–258. DOI 10.1016/j.polymer.2016.07.070.
20. Schawe, J. E. K. (2015). Analysis of non-isothermal crystallization during cooling and reorganization during heating of isotactic polypropylene by fast scanning DSC. *Thermochimica Acta*, 603, 85–93. DOI 10.1016/j.tca.2014.11.006.
21. Parija, S., Bhattacharyya, A. R. (2017). Multiwalled carbon nanotubes-based polypropylene composites: Influence of interfacial interaction on the crystallization behavior of polypropylene. *Polymer Engineering and Science*, 57(2), 183–196. DOI 10.1002/pen.24399.
22. Wang, H. Q., Li, Z. W., Hong, K. L., Chen, M. N., Qiao, Z. et al. (2019). Property improvement of multi-walled carbon nanotubes/polypropylene composites with high filler loading via interfacial modification. *RSC Advances*, 9(50), 29087–29096. DOI 10.1039/C9RA05493F.